International Journal of Applied Earth Observation and Geoinformation 13 (2011) 52–58

Contents lists available at ScienceDirect

International Journal of Applied Earth Observation and Geoinformation

journal homepage: www.elsevier.com/locate/jag

A time-integrated MODIS burn severity assessment using the multi-temporal differenced normalized burn ratio ($dNBR_{MT}$)

S. Veraverbeke[a,*], S. Lhermitte[b], W.W. Verstraeten[c], R. Goossens[a]

[a] Department of Geography, Ghent University, Krijgslaan 281 S8, BE-9000 Ghent, Belgium
[b] Centro de Estudios Avanzados en Zonas Aridas, Universidad de la Serena, Campus A. Bello, ULS, Chile
[c] Department of Biosystems, Katholieke Universiteit Leuven, Willem de Croylaan 34, BE-3001, Belgium

ARTICLE INFO

Article history:
Received 3 December 2009
Accepted 10 June 2010

Keywords:
Differenced normalized burn ratio
Fire severity
Burn severity
MODIS
Landsat Thematic Mapper
Composite burn index
Multi-temporal
Vegetation regeneration

ABSTRACT

Burn severity is an important parameter in post-fire management. It incorporates both the direct fire impact (vegetation depletion) and ecosystem responses (vegetation regeneration). From a remote sensing perspective, burn severity is traditionally estimated using Landsat's differenced normalized burn ratio (dNBR). In this case study of the large 2007 Peloponnese (Greece) wildfires, Landsat dNBR estimates correlated reasonably well with Geo composite burn index (GeoCBI) field data of severity ($R^2 = 0.56$). The usage of Landsat imagery is, however, restricted by cloud cover and image-to-image normalization constraints. Therefore a multi-temporal burn severity approach based on coarse spatial, high temporal resolution moderate resolution imaging spectroradiometer (MODIS) imagery is presented in this study. The multi-temporal dNBR ($dNBR_{MT}$) is defined as the 1-year integrated difference between burned pixels and their unique control pixels. These control pixels were selected based on time series similarity and spatial context and reflect how burned pixels would have behaved in the case no fire had occurred. Linear regression between downsampled Landsat dNBR and $dNBR_{MT}$ estimates resulted in a moderate-high coefficient of determination $R^2 = 0.54$. $dNBR_{MT}$ estimates are indicative for the change in vegetation productivity due to the fire. This change is considerably higher for forests than for more sparsely vegetated areas like shrub lands. Although Landsat dNBR is superior for spatial detail, MODIS-derived $dNBR_{MT}$ estimates present a valuable alternative for burn severity mapping at continental to global scale without image availability constraints. This is beneficial to compare trends in burn severity across regions and time. Moreover, thanks to MODIS's repeated temporal sampling, the $dNBR_{MT}$ accounts for both first- and second-order fire effects.

1. Introduction

Biomass burning is a major disturbance in almost all terrestrial ecosystems (Pausas, 2004; Riano et al., 2007). At landscape level, wildland fires partially or completely remove the vegetation layer and affect post-fire vegetation composition (Epting and Verbyla, 2005). The fire-induced vegetation depletion causes abrupt changes in carbon, energy and water fluxes at local scale (Amiro et al., 2006), thereby influencing species richness, habitats and community composition (Capitaino and Carcaillet, 2008). Accurate estimates of post-fire effects are therefore of paramount importance. To name these post-fire effects the terms fire severity and burn severity are often interchangeably used (Keeley, 2009) describing the amount of damage (Chafer, 2008), the physical, chemical and biological changes (Lee et al., 2008) or the degree of alteration (Eidenshink et al., 2007) that fire causes to an ecosystem. Some authors, however, suggest a clear distinction between both terms by considering the fire disturbance continuum (Jain et al., 2004), which addresses three different temporal fire effects phases: before, during and after the fire. In this context, fire severity quantifies the short-term fire effects in the immediate post-fire environment whereas burn severity quantifies both the short- and long-term impact as it includes response processes (e.g. resprouting, delayed mortality; Lentile et al., 2006; Key, 2006). Fig. 1 represents a summary of post-fire effects terminology.

In remote sensing studies burn severity is traditionally estimated using Landsat imagery (Key and Benson, 2005; French et al., 2008). A popular approach, partly because of its conceptual simplicity, can be found in rationing band reflectance data. In this respect the normalized burn ratio (NBR) has become accepted as the standard spectral index to assess burn severity (Lopez-Garcia and Caselles, 1991; Key and Benson, 2005; French et al., 2008; Veraverbeke et al., in press-a). The NBR relates to vegetation moisture content by combining the near infrared (NIR) and mid infrared

* Corresponding author. Tel.: +32 9 2644646; fax: +32 9 2644985.
E-mail address: sander.veraverbeke@ugent.be (S. Veraverbeke).

0303-2434/$ – see front matter © 2010 Elsevier B.V. All rights reserved.
doi:10.1016/j.jag.2010.06.006

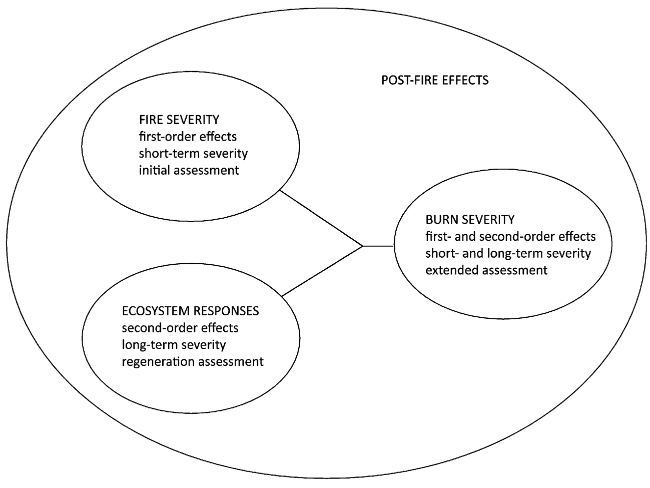

Fig. 1. Schematic representation of post-fire effects terminology (Veraverbeke et al., in press-a).

(MIR) spectral regions. Generally, pre- and post-fire NBR images are bi-temporally differenced, resulting in the differenced NBR (dNBR).

The dNBR method relies on Landsat imagery and thus depends on image availability, which is limited to infrequent images over small areas due to Landsat's 16-day revisiting cycle and cloud cover (Ju and Roy, 2008). Bi-temporal studies are even more hampered as they require an effective image-to-image normalization (Coppin et al., 2004) including the removal of phenological, atmospheric and bi-directional reflectance distribution function (BRDF) effects (Verbyla et al., 2008; Veraverbeke et al., 2010). As a result Landsat-based burn severity studies have proven to be valuable for obtaining detailed information over specific fires, however, the magnitude of the observed dNBR change heavily depends on assessment timing (Key, 2006; Veraverbeke et al., in press-b). This temporal dissimilarity limits the comparison between bi-temporal dNBR assessments of different fires (Eidenshink et al., 2007; Verbyla et al., 2008), especially when a comparison between different ecoregions is required (Eidenshink et al., 2007; French et al., 2008). The use of high temporal, coarse spatial resolution data possibly provides a sound alternative to Landsat dNBR estimates. In addition, their repeated temporal sampling allows quantifying both the direct fire impact and regeneration processes. To date few studies have implemented coarse resolution time series to assess burn severity. In this context it is worth mentioning the effort of Lhermitte et al. (in review), who illustrated the potential of time series data to account for inter- and intra-annual post-fire vegetation dynamics. In their method each burned pixel is compared with an unburned control pixel. These control pixels were selected based on pre-fire time series similarity and spatial context.

The aim of this study is to present a multi-temporal dNBR ($dNBR_{MT}$) burn severity assessment as an alternative for traditional Landsat dNBR mapping. The method incorporates both the direct fire impact and vegetation regeneration (Lentile et al., 2006). Moderate resolution imaging spectroradiometer (MODIS) time series are used over the large 2007 Peloponnese (Greece) wildfires. $dNBR_{MT}$ estimates are compared with Landsat and field data.

2. Data and study area

2.1. Study area

The study area is situated at the Peloponnese peninsula, in southern Greece (36°30′–38°30′N, 21°–23°E) (see Fig. 2). The topography is rugged with elevations ranging between 0 and 2404 m above sea level. The climate is typically Mediterranean with hot, dry summers and mild, wet winters. For the Kalamata meteorological station (37°4′N, 22°1′E) the average annual temperature is 17.8 °C and the mean annual precipitation equals 780 mm.

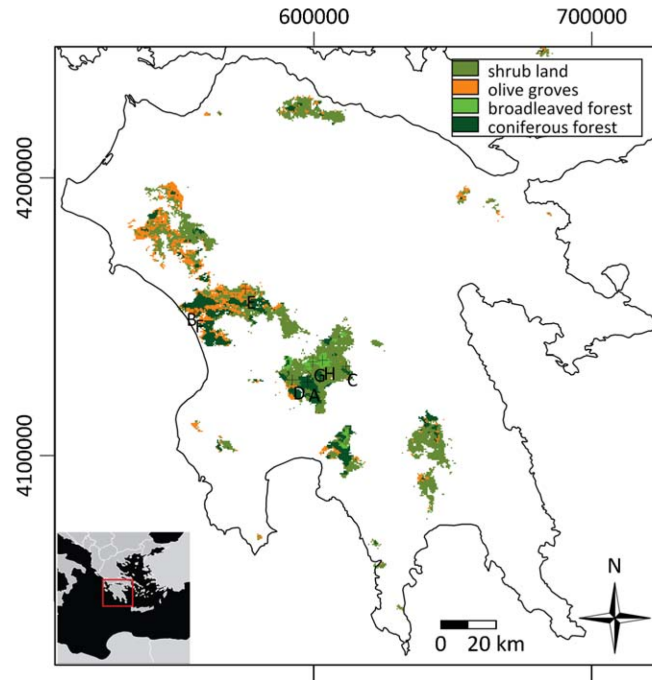

Fig. 2. Pre-fire land cover types of the burned areas (Veraverbeke et al., in press-a). The locations of the example pixels shown in Fig. 7 are also indicated (A–H).

After a severe drought period several large wildfires of unknown cause have struck the area in the 2007 summer. The fires were the worst natural disaster of the last decades in Greece, both in terms of human losses and the extent of the burned area. The fires consumed more than 175 000 ha, which consisted of 57% shrub land, 21% coniferous forest, 20% olive groves and 2% broadleaved forest (Veraverbeke et al., in press-b).

2.2. Field data

150 Geo composite burn index (GeoCBI) plots were sampled 1 year post-fire, in September 2008. The GeoCBI is a modification of the composite burn index (CBI) (De Santis and Chuvieco, 2009). It is an operational tool used in conjunction with the Landsat dNBR approach to assess burn severity in the field (Key and Benson, 2005). The GeoCBI divides the ecosystem into five different strata, one for the substrates and four vegetation layers. These strata are: (i) substrates, (ii) herbs, low shrubs and trees less than 1 m, (iii) tall shrubs and trees of 1–5 m, (iv) intermediate trees of 5–20 m and (v) big trees higher than 20 m. In the field form, 20 different factors can be rated (e.g. soil and rock cover/color change, % LAI change, char height) but only those factors present and reliably rateable, are considered. The rates are given on a continuous scale between zero and three and the resulting factor ratings are averaged per stratum. Based on these stratum averages, the GeoCBI is calculated in proportion to their corresponding fraction of cover, resulting in a weighted average between zero and three that expresses burn severity. As the field data were collected 1 year post-fire, it is an extended assessment. Additional information on the field data can be found in Veraverbeke et al. (in press-b).

2.3. Landsat data

For the traditional Landsat dNBR assessment two anniversary date Thematic Mapper (TM) images (path/row 184/34) were used (23/07/2006 and 13/08/2008). In correspondence with the timing of the field sampling, the post-fire image was acquired 1 year post-fire. The images were acquired in the summer, minimizing effects of vegetation phenology and differing solar zenith angles. The images were subjected to geometric, radiometric, atmospheric and topographic correction.

The 2008 image was geometrically corrected using 34 ground control points (GCPs), recorded in the field with a Garmin eTrex Vista GPS (15 m error in x and y (Garmin, 2005)). The resulting root mean squared error (RMSE) was lower than 0.5 pixels. The 2006 and 2008 images were co-registered within 0.5 pixels accuracy. The images were registered in UTM (zone 34S), with the World Geodetic System 84 (WGS-84) as geodetic datum.

Raw digital numbers (DNs) were scaled to at-sensor radiance values (L_s) (Chander et al., 2007). The radiance to reflectance conversion was performed using the COST method (Chavez, 1996):

$$\rho_a = \frac{\pi(L_s - L_d)}{(E_0/d^2)(\cos\theta_z)^2} \tag{1}$$

where ρ_a is the atmospherically corrected reflectance at the surface; L_s is the at-sensor radiance (W m^{-2} sr^{-1}); L_d is the path radiance (W m^{-2} sr^{-1}); E_0 is the solar spectral irradiance (W m^{-2}); d is the earth–sun distance (astronomical units); θ_z is the solar zenith angle. The COST method is a dark object subtraction (DOS) approach that assumes 1% surface reflectance for dark objects (e.g. deep water). After applying the COST atmospheric correction, pseudo-invariant features (PIFs) such as deep water and bare soil pixels, were examined in the images. No further relative normalization between the images was required.

It was necessary to correct for different illumination effects due to topography as the common assumption that shading effects are removed in ratio-based analyses does not necessarily hold true (Verbyla et al., 2008; Veraverbeke et al., 2010). This was done based on the modified C correction method (Veraverbeke et al., 2010), a modification of the original C correction approach (Teillet et al., 1982), using a DEM and knowledge of the solar zenith and azimuth angle at the moment of image acquisition. Topographical slope and aspect data were derived from 90 m shuttle radar topographic mission (SRTM) elevation data (Jarvis et al., 2006) resampled and co-registered with the Landsat images. The illumination is modeled as:

$$\cos\gamma_i = \cos\theta_p \cos\theta_z + \sin\theta_p \sin\theta_z \cos(\phi_a - \phi_0) \tag{2}$$

where γ_i is the incident angle (angle between the normal to the ground and the sun rays); θ_p is the slope angle; θ_z is the solar zenith angle; ϕ_a is the solar azimuth angle; ϕ_0 is the aspect angle. Then terrain corrected reflectance ρ_t is defined as:

$$\rho_t = \rho_a \left(\frac{1 + c_k}{\cos\gamma_i + c_k}\right) \tag{3}$$

where c_k is a band specific parameter $c_k = b_k/m_k$ where b_k and m_k are the respective intercept and slope of the regression equation $\rho_a = b_k + m_k \cos\gamma_i$.

Finally, by inputting the NIR (TM4: centered at 830 nm) and MIR (TM7: centered at 2215 nm) bands NBR and dNBR images were generated:

$$\mathrm{NBR} = \frac{\mathrm{NIR} - \mathrm{MIR}}{\mathrm{NIR} + \mathrm{MIR}}, \qquad \mathrm{dNBR} = \mathrm{NBR}_{\mathrm{pre}} - \mathrm{NBR}_{\mathrm{post}} \tag{4}$$

2.4. MODIS data

Level 2 daily Terra MODIS surface reflectance (500 m) tiles (MOD09GA) including associated quality assurance (QA) layers were acquired from the national aeronautics and space administration (NASA) warehouse inventory search tool (WIST) (http://wist.echo.nasa.gov) for the period 01/01/2006 till 31/12/2008. These products contain an estimate of the surface reflectance for seven optical bands as it would have been measured at ground level as if there were no atmospheric scattering or absorption (Vermote et al., 2002). The data preprocessing steps included subsetting, reprojecting, compositing, creating continuous time series and indexing. The study area was clipped and the NIR (centered at 858 nm), MIR (centered at 2130 nm) and QA layers were reprojected into UTM with WGS 84 as geodetic datum. Subsequently, the daily NIR, MIR and QA data were converted in 8-day composites using the minimum NIR criterion to minimize cloud contamination and off-nadir viewing effects (Holben, 1986). The minimum NIR criterion has proven to allow a more accurate discrimination between burned and unburned pixels than traditional maximum value composites (MVCs) (Chuvieco et al., 2005). After compositing bad QA observations were replaced by a Savitzky–Golay filter as implemented in the TIMESAT software (Jonsson and Eklundh, 2004). The TIMESAT program allows the inclusion of a preprocessing mask that determines the uncertainty of data values. Cloud-affected observations were identified using the internal cloud and cloud-adjacency algorithm flags of the QA layer. These flags consist of binary layers which permit to assign a zero weight value to cloudy and cloud-adjacent observations. Consequently, these data do not influence the filter procedure. Only the values of the masked observations were replaced to retain as much as possible the original NIR and MIR reflectance values. Finally, the NBR index was calculated as using Eq. (4).

2.5. Control pixel data

Control pixel data were retrieved making use of pre-fire time series similarity and spatial context (Lhermitte et al., 2010) as implemented in Veraverbeke et al. (in press-b). The control pixel selection procedure assigns a unique control pixel to each burned pixel. This is done based on time series similarity between a burned pixel and its closest unburned neighbor pixels during a pre-fire period. To quantify dissimilarity the averaged Euclidian distance dissimilarity criterion D was used:

$$D = \frac{\sqrt{\sum_{t=1}^{N} (\mathrm{NBR}_t^f - \mathrm{NBR}_t^x)^2}}{N} \tag{5}$$

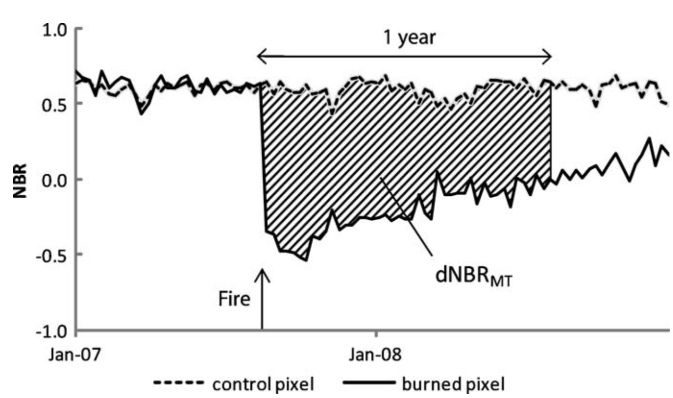

Fig. 3. Principle of the multi-temporal dNBR (dNBR$_{MT}$). The dNBR$_{MT}$ represents the averaged integrated difference between the 1-year post-fire NBR time series of the control and focal pixels, as shown in the figure by the shaded area.

where NBR_t^f and NBR_t^x are the respective burned focal and unburned candidate control pixel time series, while N is the number of observations in pre-fire year ($N = 46$). The Euclidian distance metric has an intuitive appeal: it quantifies the straight line inter-point distance in a multi-temporal space as distance measure. As a result, it is robust for both data space translations and rotations. Consequently, it is a very useful metric to assess inter-pixel differences in time series (Lhermitte et al., 2010). In this approach the averaged time series from the four most similar out of eight candidate pixels defines the control pixel time series. This setting accounts for both a beneficial averaging effect and the advantage of spatial proximity (Veraverbeke et al., in press-b). The resulting control pixels reflect the vegetation dynamics of each burned pixel in case that there would not have occurred a fire. Additional information on the control plot selection procedure can be found in Lhermitte et al. (2010) and Veraverbeke et al. (in press-b).

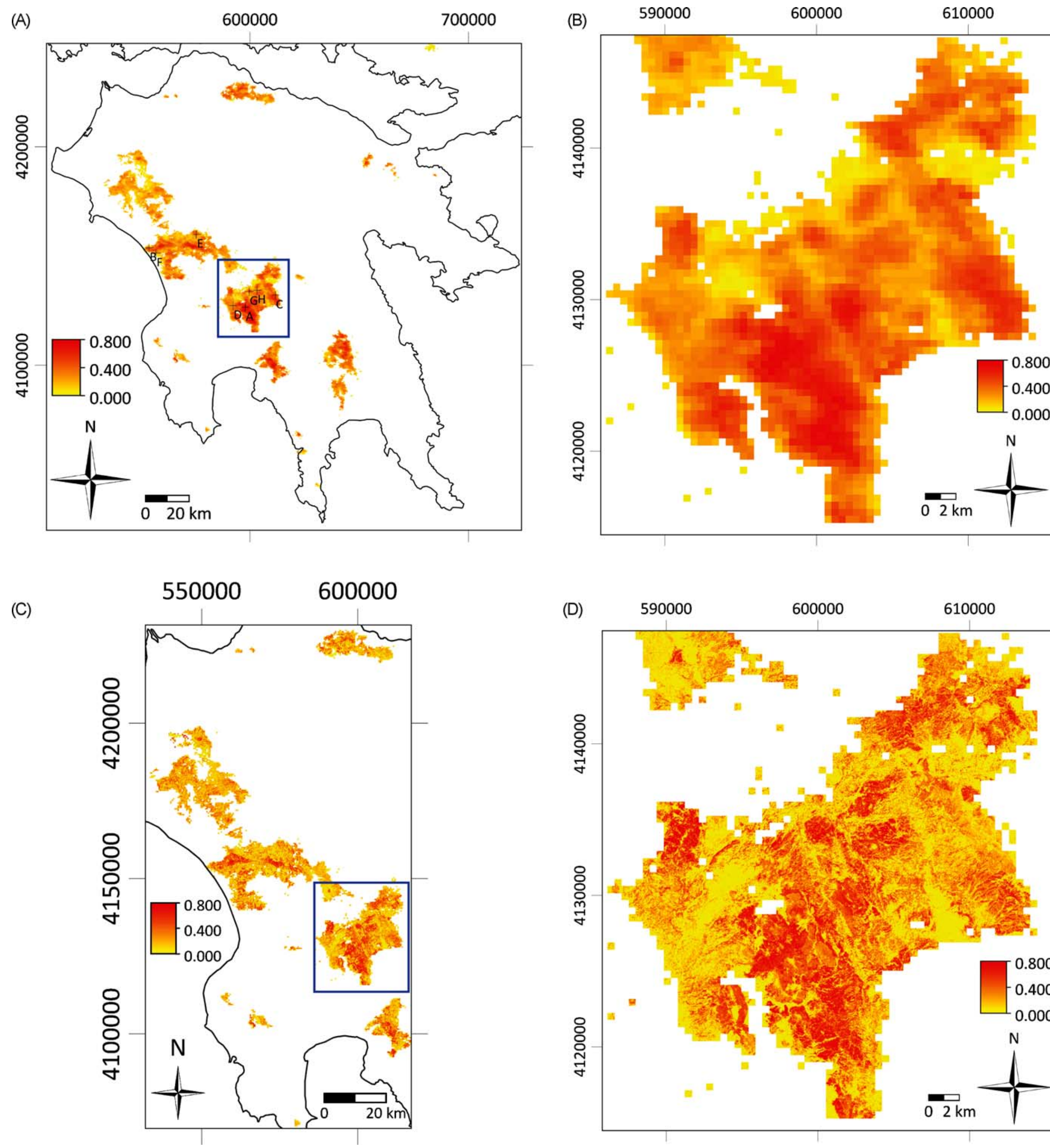

Fig. 4. MODIS $dNBR_{MT}$ map (A), subset MODIS $dNBR_{MT}$ map of the blue rectangle in (A) (B), Landsat dNBR map (C) and subset Landsat dNBR map of the blue rectangle in (C) (D). The locations of the example pixels shown in Fig. 7 are also indicated in (A). (For interpretation of the references to color in this figure legend, the reader is referred to the web version of the article.)

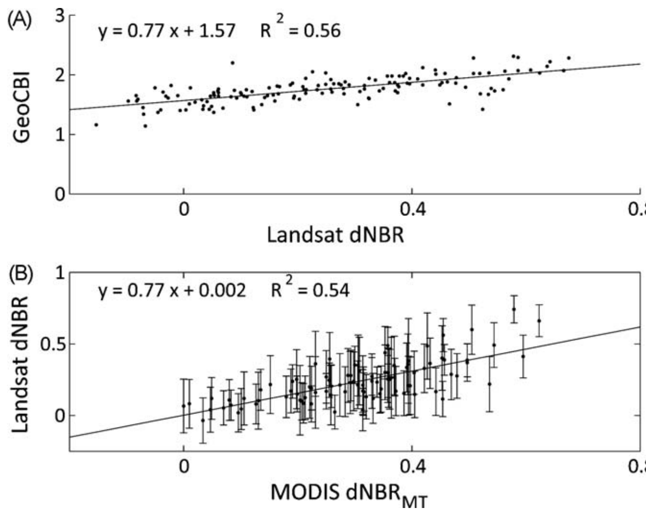

Fig. 5. Scatter plot and regression line between Landsat dNBR and GeoCBI (A) and between MODIS dNBR_{MT} and Landsat dNBT (B) (n = 150, p < 0.001). The vertical bars in B indicate the standard deviation of Landsat pixels within one MODIS pixel.

3. Methodology

Burn severity incorporates both short- and long-term post-fire effects on the environment (Lentile et al., 2006). Consequently, burn severity is a combination of immediate fire impact and the ecosystem's ability to regenerate. Based on these characteristics, we propose a multi-temporal dNBR (dNBR_{MT}) that integrates the difference between the NBR values of a burned pixel and its corresponding control pixel over time. Doing so the dNBR_{MT} is defined as:

$$\text{dNBR}_{\text{MT}} = \frac{\sum_{t=1}^{N}(\text{NBR}_t^f - \text{NBR}_t^c)}{N} \tag{6}$$

where NBR_t^f and NBR_t^c are the respective burned focal and unburned control pixel observations, while N is the number of post-fire observations included in the study (here N = 46 for 1 year) and t = 1 is the first post-fire observation. Fig. 3 illustrates the principle of the dNBR_{MT}. Dividing by the number of post-fire observations N normalizes the dNBR_{MT} data to the same range as bi-temporal dNBR assessments. dNBR_{MT} estimates will show large positive values for high burn severity. The application of an integral has been used to characterize vegetation productivity (Reed et al., 1994; Heumann et al., 2007). The integrated change between NBR values of control and burned pixels is therefore indicative for the change in vegetation productivity caused by the fire. To evaluate the performance of the multi-temporal approach comparison is made with a traditional Landsat TM dNBR assessment and GeoCBI field data.

4. Results

Fig. 4A shows the result of the MODIS dNBR_{MT} approach, while Fig. 4B details a specific burned area framed in blue in Fig. 4A. Fig. 4C displays the traditional Landsat dNBR, while Fig. 4D also depicts the detailed subset. On a coarse scale the MODIS and Landsat assessments reveal the same patterns of burn severity, however, it is trivial that Landsat estimates are characterized by more spatial detail. This is also visible in Fig. 5. The scatter plot between GeoCBI and Landsat dNBR estimates is given in Fig. 5A. The linear regression fit resulted in a coefficient of determination R^2 = 0.56. Fig. 5B presents the scatter plot between downsampled Landsat data and corresponding dNBR_{MT} estimates for the 150 field-sampled locations. The vertical bars indicate the standard deviation (sd) of the Landsat pixels within one MODIS pixel. Although the correlation between downsampled Landsat dNBR and MODIS dNBR_{MT} estimates is moderately high (R^2 = 0.54), it is clear that there exists considerable variation within one MODIS pixel (sd of Landsat dNBR up to 0.25).

In Fig. 6 mean dNBR_{MT} (sd) is plotted per land cover type. One can clearly see that the 1-year integrated change is higher for forests than for more sparsely vegetated covers. dNBR_{MT} estimates are the highest for coniferous forest, followed by broadleaved forest. Shrub land and olive groves have considerably lower dNBR_{MT} estimates. Fig. 7 examples temporal profiles of eight pixels. These figures demonstrate that dNBR_{MT} estimates account for both the direct fire impact and the ability to recover.

5. Discussion

A major advantage of the multi-temporal burn severity approach is its combination of both the immediate fire impact and vegetation regrowth. As such, it is more tightly connected to the definition of burn severity. Key and Benson (2005) stated that burn severity encloses both first- and second-order fire effects. The most important first-order effect is the fire's vegetation consumption, while vegetation regeneration and delayed mortality are substantial second-order effects. In that respect, Lentile et al. (2006) specified that burn severity relates to the amount of time

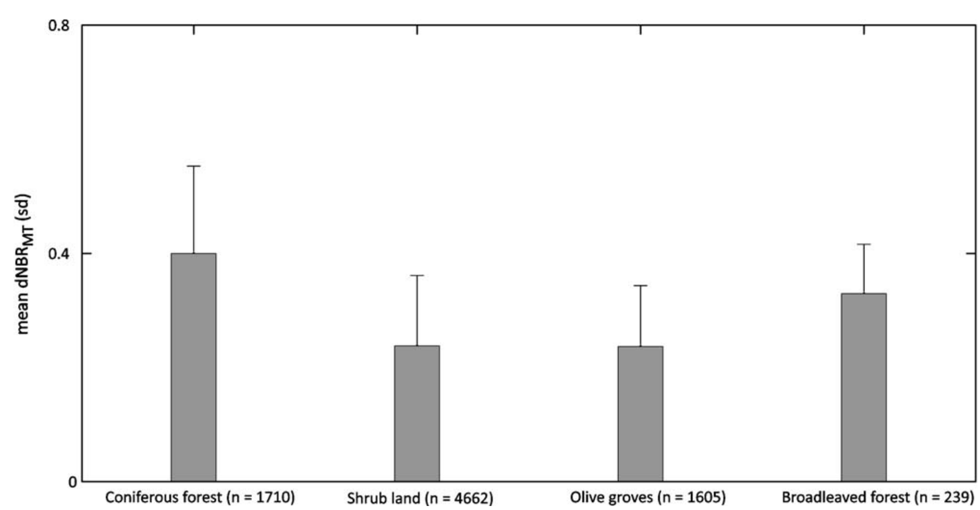

Fig. 6. Mean dNBR_{MT} and standard deviation per land cover type.

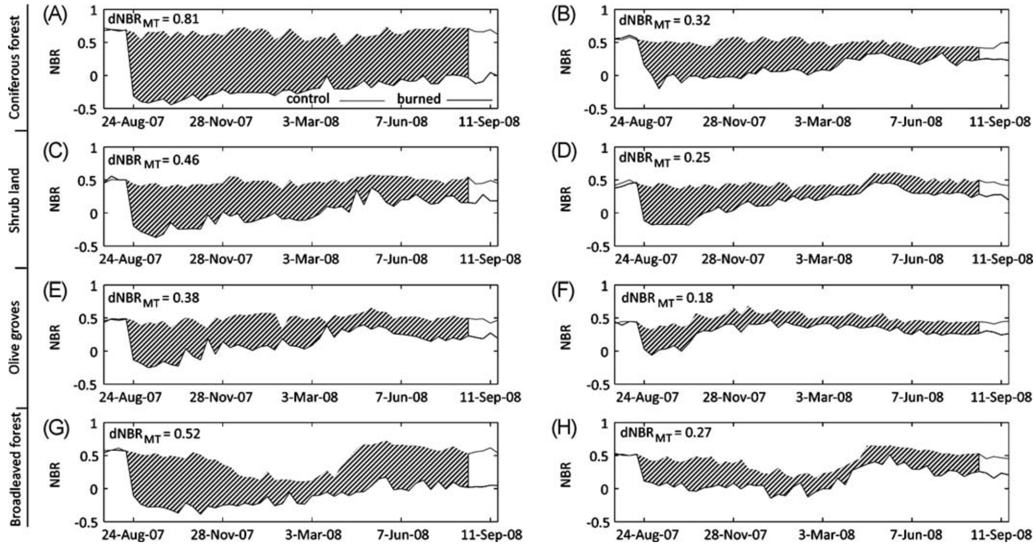

Fig. 7. Illustration of $dNBR_{MT}$ estimates (shaded area) for coniferous forest (A and B), shrub land (C and D), olive groves (E and F) and broadleaved forest (G and H). The location of the pixels is given in Figs. 2 and 4A.

necessary to return to pre-fire level. As a consequence plots that experienced a high fire severity and fast regeneration will result in similar $dNBR_{MT}$ outcomes as plots that were only slightly affected by the fire but with slow recovery. While in some studies it can be important to distinguish between first- and second-order effects, burn severity incorporates both (Lentile et al., 2006; Keeley, 2009). The application of an integral has been used to characterize vegetation productivity (Reed et al., 1994; Heumann et al., 2007). As such, the integrated change between NBR values of control and burned pixels, as gauged by the $dNBR_{MT}$, reflects the change in productivity due to the fire. Seasonality and recovery processes vary per land cover type (Reed et al., 1994; White et al., 1996). As a result, $dNBR_{MT}$ estimates are clearly higher for forests than for more sparsely vegetated areas (Figs. 6 and 7). Recovery in forests can take several decades (Nepstad et al., 1999), whereas shrub species are typified by a relatively fast recovery (Keeley et al., 2005). The $dNBR_{MT}$ incorporates this difference. Moreover, depending on the application and the ecotype, one could decide to alter the integration period (1 year in this study).

In corroboration with previous findings (French et al., 2008), Landsat dNBR correlated reasonably well with field data of severity. The correlation between GeoCBI and Landsat data differed from previously published outcomes based on the same data (Veraverbeke et al., in press-a), mainly because of some minor changes in satellite preprocessing and the exclusion of ten unburned field plots. Multi-temporal MODIS burn severity estimates showed a moderate-high correlation with the dNBR of a traditional bi-temporal Landsat assessment ($R^2 = 0.54$). The slope of the regression equation (0.77) was considerably lower than one. In contrast with the 1-year post-fire Landsat assessment, $dNBR_{MT}$ estimates also incorporate observations from the immediate post-fire period. As a consequence $dNBR_{MT}$ estimates were slightly higher than the Landsat dNBR. Despite of the coarse scale resemblance between Landsat and MODIS data, Landsat data are superior to reveal spatial detail (Hilker et al., 2009). These data, however, fail to comprehend the temporal dimension of burn severity. Moreover, the magnitude of change measured with the traditional Landsat dNBR highly depends on assessment timing (Key, 2006; Veraverbeke et al., in press-b). Allen and Sorbel (2008), for example, found that initial and extended assessments produced significantly different information with regards to burn severity for tundra vegetation, while the timing of the assessment had no effect for back spruce forest, which was attributed to the rapid tundra recovery. Verbyla et al. (2008) reported a seasonality effect that resulted in large dissimilarities in dNBR values for only slightly differing assessment timings, probably due to a combined effect of senescing vegetation and changing illumination conditions. Veraverbeke et al. (2010) illustrated the necessity to correct for illumination effects, also in a ratio-based NBR analysis, because these effects affected the performance of the dNBR, even for bi-temporal acquisitions schemes that only slightly deviated from the ideal anniversary date scheme. This timing constraint potentially hampers the comparison of Landsat dNBR estimates across region and time (Eidenshink et al., 2007; Verbyla et al., 2008). If the period of the $dNBR_{MT}$'s integration remains the same for different fires, the multi-temporal approach truly has the potential to allow a better comparison of burn severity either in time or space. Thus, where fine resolution Landsat studies allow revealing high spatial detail, which is favorable for regional studies, their usage is limited due cloud cover problems (Ju and Roy, 2008) and difficulties in image-to-image normalization (Coppin et al., 2004; Verbyla et al., 2008; Veraverbeke et al., 2010). Therefore, the high temporal frequency of coarse resolution imagery can either be a vital complement to traditional Landsat dNBR mapping of specific fires or an imperative alternative for the assessment of burn severity at continental to global scales.

6. Conclusions

In this study a multi-temporal method to assess burn severity of the 2007 Peloponnese (Greece) wildfires has been proposed. The approach introduces an alternative for traditional Landsat dNBR mapping, which can be constrained due to cloud cover and image-to-image normalization difficulties. The method is based on coarse spatial resolution with high temporal frequency MODIS imagery. MODIS's daily MIR and NIR reflectance products were first composited in 8-day periods and missing values were replaced. Subsequently, for each burned pixel a unique control pixel has been retrieved based on time series similarity and spatial context. The $dNBR_{MT}$ was then calculated as the 1-year post-fire integrated difference between the NBR of the control and burned pixels, averaged by the total number of observations. $dNBR_{MT}$ estimates reflect the change in vegetation productivity caused by the fire. This change is clearly higher for forests than for shrub lands. By integrating over time, $dNBR_{MT}$ estimates account for both the direct fire impact and ecosystem responses. As such the $dNBR_{MT}$ is more tightly connected to the definition of burn severity compared to traditional bi-temporal Landsat dNBR mapping. $dNBR_{MT}$ estimates correlated reasonably well with the downsampled Landsat dNBR, which on its turn showed a moderate-high correlation with GeoCBI field data. Although Landsat dNBR is superior for spatial detail in regional scale studies, the $dNBR_{MT}$ presents a valuable alternative for burn severity mapping at a regional to global scale. The approach also has potential to enhance comparability of different fires across regions and time.

Acknowledgements

The study was financed by the Ghent University special research funds (BOF: Bijzonder Onderzoeksfonds). The authors would like to thank the anonymous reviewers for their constructive remarks.

References

Allen, J., Sorbel, B., 2008. Assessing the differenced normalized burn ratio's ability to map burn severity in the boreal forest and tundra ecosystems of Alaska's national parks. Int. J. Wildland Fire 17, 463–475.

Amiro, B., Barr, A., Black, T., Iwashita, H., Kljun, N., McCaughey, J., Morgenstern, K., Muruyama, S., Nesic, Z., Orchansky, A., Saigusa, N., 2006. Carbon, energy and water fluxes at mature and disturbed forest sites, Saskatchewan, Canada. Agric. Forest Meteorol. 136, 237–251.

Capitaino, R., Carcaillet, C., 2008. Post-fire Mediterranean vegetation dynamics and diversity: a discussion of succession models. Forest Ecol. Manage. 255, 431–439.

Chafer, C., 2008. A comparison of fire severity measures: an Australian example and implications for predicting major areas of soil erosion. Catena 74, 235–245.

Chander, G., Markham, L., Barsi, J., 2007. Revised Landsat-5 Thematic Mapper radiometric calibration. IEEE Geosci. Remote Sens. Lett. 4, 490–494.

Chavez, P., 1996. Image-based atmospheric corrections—revisited and improved. Photogramm. Eng. Remote Sens. 6, 1025–1036.

Chuvieco, E., Ventura, G., Martin, P., Gomez, I., 2005. Assessment of multitemporal compositing techniques of MODIS and AVHRR images for burned land mapping. Remote Sens. Environ. 94, 450–462.

Coppin, P., Jonckheere, I., Nackaerts, K., Muys, B., 2004. Digital change detection techniques in ecosystem monitoring: a review. Int. J. Remote Sens. 25, 1565–1595.

De Santis, A., Chuvieco, E., 2009. GeoCBI: a modified version of the composite burn index for the initial assessment of the short-term burn severity from remotely sensed data. Remote Sens. Environ. 113, 554–562.

Eidenshink, J., Schwind, B., Brewer, K., Zhu, Z., Quayle, B., Howard, S., 2007. A project for monitoring trends in burn severity. Fire Ecol. 3, 3–21.

Epting, J., Verbyla, D., 2005. Landscape-level interactions of prefire vegetation, burn severity, and postfire vegetation over a 16-year period in interior Alaska. Can. J. Forest Res. 35, 1367–1377.

French, N., Kasischke, E., Hall, R., Murphy, K., Verbyla, D., Hoy, E., Allen, J., 2008. Using Landsat data to assess fire and burn severity in the North American boreal forest region: an overview and summary of results. Int. J. Wildland Fire 17, 443–462.

Garmin, 2005. Garmin eTrex Vista Personal Navigator. Owner's Manual and Reference Guide, Available from: http://buy.garmin.com/shop/store/manual.jsp?product=010-00243-00&cID=167&pID=163 (Last visited on 22/04/2010).

Heumann, B., Seaquist, J., Eklundh, L., Jonsson, P., 2007. AVHRR derived phenological change in the Sahel and Soudan, Africa, 1982–2005. Remote Sens. Environ. 108, 385–392.

Hilker, T., Wulder, M., Coops, N., Linke, J., McDermid, G., Masek, J., Gao, F., White, J., 2009. A new data fusion model for high spatial- and temporal-resolution mapping of forest disturbance based on Landsat and MODIS. Remote Sens. Environ. 113, 1623–1627.

Holben, B., 1986. Characteristics of maximum-value composite images from temporal AVHRR data. Int. J. Remote Sens. 7, 1417–1434.

Jain, T., Pilliod, D., Graham, R., 2004. Tongue-tied. Wildfire 4, 22–26.

Jarvis, A., Reuter, H., Nelson, A., Guevara, E., 2006. Hole-filled Seamless SRTM Data V3, Available from: http://srtm.csi.cgiar.org (Last visited on 22/04/2010).

Jonsson, P., Eklundh, L., 2004. TIMESAT-a program for analyzing time-series of satellite sensor data. Comput. Geosci. 30, 833–845.

Ju, J., Roy, D., 2008. The availability of cloud-free Landsat ETM+ data over the conterminous United States and globally. Remote Sens. Environ. 112, 1196–1211.

Keeley, J., 2009. Fire intensity, fire severity and burn severity: a brief review and suggested usage. Int. J. Wildland Fire 18, 116–126.

Key, C., Benson, N., 2005. Landscape assessment: ground measure of severity; the composite burn index, and remote sensing of severity, the normalized burn index. In: Lutes, D., Keane, R., Caratti, J., Key, C., Benson, N., Sutherland, S., Gangi, L. (Eds.), FIREMON: Fire Effects Monitoring and Inventory System. USDA Forest Service, Rocky Mountains Research Station, General Technical Report RMRS-GTR-164-CD LA, pp. 1–51.

Keeley, J., Fotheringham, C., Bear-Keeley, M., 2005. Factors affecting plant diversity during post-fire recovery and succession of mediterranean-climate shrublands in California, USA. Divers. Distrib. 11, 525–537.

Key, C., 2006. Ecological and sampling constraints on defining landscape fire severity. Fire Ecol. 2, 34–59.

Lee, B., Kim, S., Chung, J., Park, P., 2008. Estimation of fire severity by use of Landsat TM images and its relevance to vegetation and topography in the 2000 Samcheok forest fire. J. Forest Res. 13, 197–204.

Lentile, L., Holden, Z., Smith, A., Falkowski, M., Hudak, A., Morgan, P., Lewis, S., Gessler, P., Benson, N., 2006. Remote sensing techniques to assess active fire characteristics and post-fire effects. Int. J. Wildland Fire 15, 319–345.

Lhermitte, S., Verbesselt, J., Verstraeten, W.W., Veraverbeke, S. Coppin, P., in review. Assessing intra-annual vegetation regrowth after fire using the pixel based regeneration index. ISPRS J. Photogramm. Remote Sens.

Lhermitte, S., Verbesselt, J., Verstraeten, W.W., Coppin, P., 2010. A pixel based regeneration index using time series similarity and spatial context. Photogramm. Eng. Remote Sens. 76, 673–682.

Lopez-Garcia, M., Caselles, V., 1991. Mapping burns and natural reforestation using Thematic Mapper data. Geocarto Int. 6, 31–37.

Nepstad, D., Verssimo, A., Alencar, A., Nobre, C., Lima, E., Lefebvre, P., Schlesinger, P., Potter, C., Moutinho, P., Mendoza, E., Cochrane, M., Brooks, V., 1999. Large-scale impoverishment of Amazonian forests by logging and fire. Nature 398, 505–508.

Pausas, J., 2004. Changes in fire and climate in the eastern Iberian peninsula (Mediterranean Basin). Clim. Change 63, 337–350.

Reed, B., Brown, J., Vanderzee, D., Loveland, T., Merchant, J., Ohlen, D., 1994. Measuring phenological variability from satellite imagery. J. Veg. Sci. 15, 703–714.

Riano, D., Moreno-Ruiz, J., Isidoros, D., Ustin, S., 2007. Global spatial patterns and temporal trends of burned area between 1981 and 2000 using NOAA-NASA Pathfinder. Glob. Change Biol. 13, 40–50.

Teillet, P., Guindon, B., Goodenough, D., 1982. On the slope-aspect correction of multispectral scanner data. Can. J. Remote Sens. 8, 84–106.

Veraverbeke, S., Verstraeten, W.W., Lhermitte, S., Goossens, R., 2010. Illumination effects on the differenced normalized burn ratio's optimality for assessing fire severity. Int. J. Appl. Earth Observation Geoinf. 12, 60–70.

Veraverbeke, S., Verstraeten, W., Lhermitte, S., Goossens, R., in press. Evaluation Landsat Thematic Mapper spectral indices for estimating burn severity of the 2007 Peloponnese wildfires in Greece. Int. J. Wildland Fire.

Veraverbeke, S., Lhermitte, S., Verstraeten, W.W., Goossens, R., in press. The temporal dimension of differenced normalized burn ratio (dNBR) fire/burn severity studies: the case of the large 2007 Peloponnese wildfires in Greece. Remote Sens. Environ.

Verbyla, D., Kasischke, E., Hoy, E., 2008. Seasonal and topographic effects on estimating fire severity from Landsat TM/ETM+ data. Int. J. Wildland Fire 17, 527–534.

Vermote, E., El Saleous, N., Justice, C., 2002. Atmospheric correction of MODIS data in the visible to middle infrared: first results. Remote Sens. Environ. 83, 97–111.

White, J., Ryan, K., Key, C., Running, S., 1996. Remote sensing of forest fire severity and vegetation recovery. Int. J. Wildland Fire 6, 125–136.